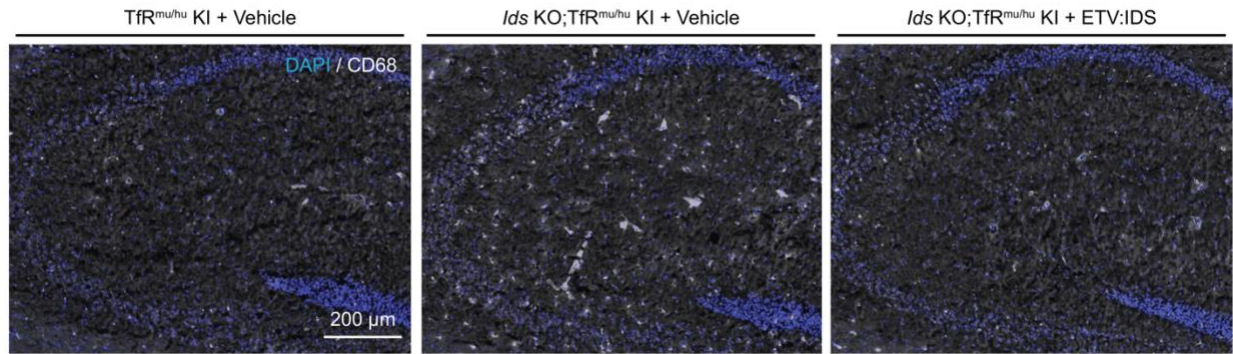
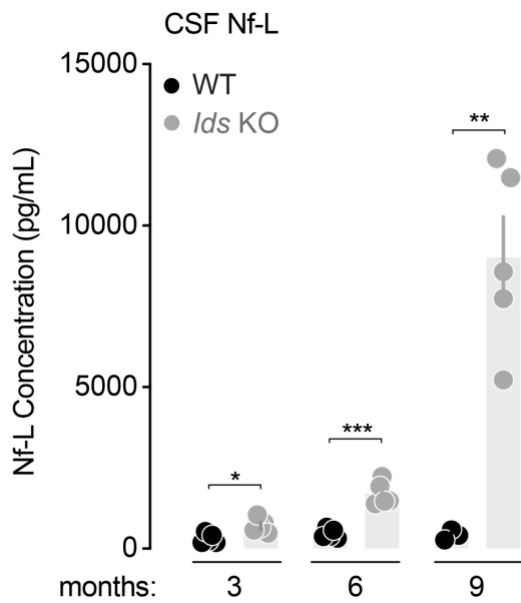


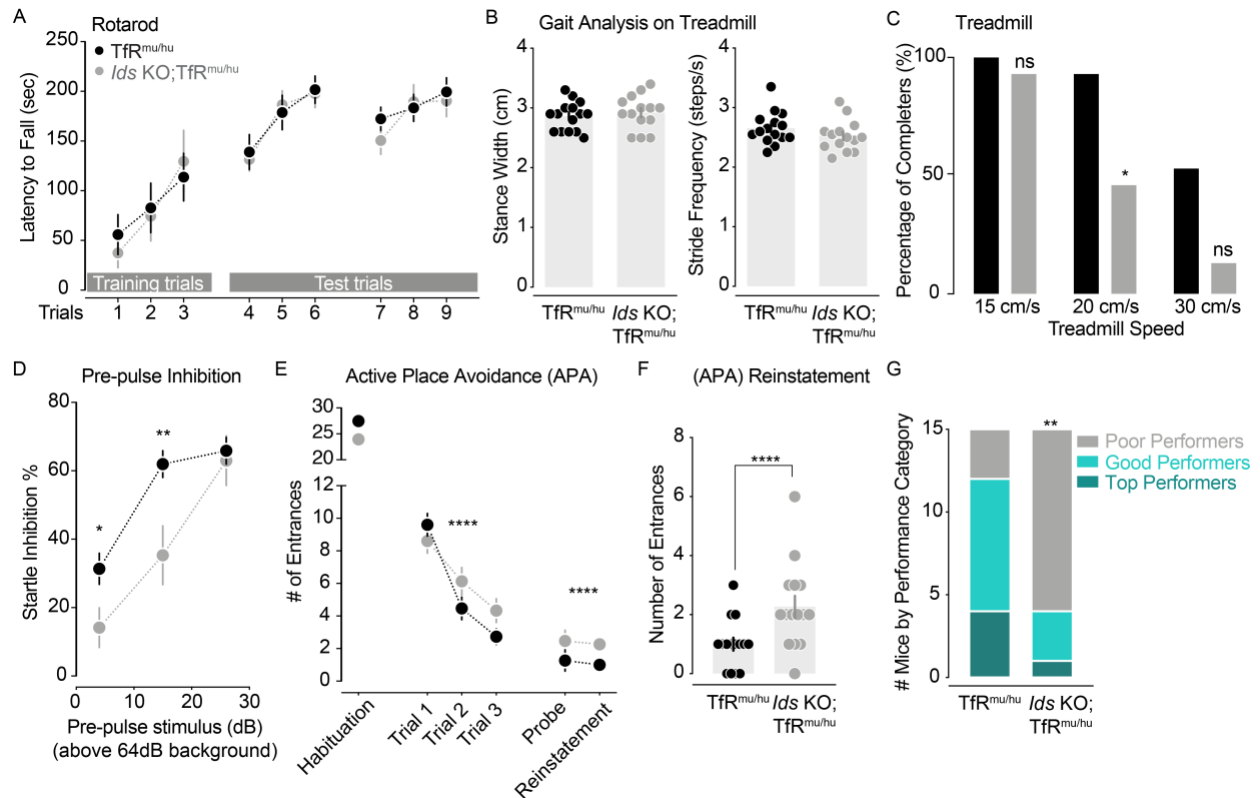
Supplemental Figure 1. Intraperitoneal (IP) delivery of ETV:IDS has a similar PK and PD response as intravenous (IV) administration. (A) Serum concentrations of ETV:IDS from *TfR^{mu/hu}* mice were measured 0.25, 1, 2, 4, 8, 24, 72, and 168 hours after a single IV or IP dose of 1 or 5 mg/kg; $n = 4$ per group. Graphs display mean \pm SD. (B) Brain concentrations of ETV:IDS were measured at 2, 8, 72, and 168 hours after a single IV or IP dose of 1 or 5 mg/kg; $n = 4$ per group. Graphs display mean \pm SD. (C) GAG levels were evaluated in the brain of *Ids KO;TfR^{mu/hu}* mice 7 days following treatment with ETV:IDS after 4 weekly IV or IP doses of 1 or 5 mg/kg and compared to vehicle treatment and non-diseased *TfR^{mu/hu}* KI mice; $n = 4-5$ per group. Graphs display mean \pm SEM and p values: one-way ANOVA with Tukey's multiple comparison test; ns = not significant.



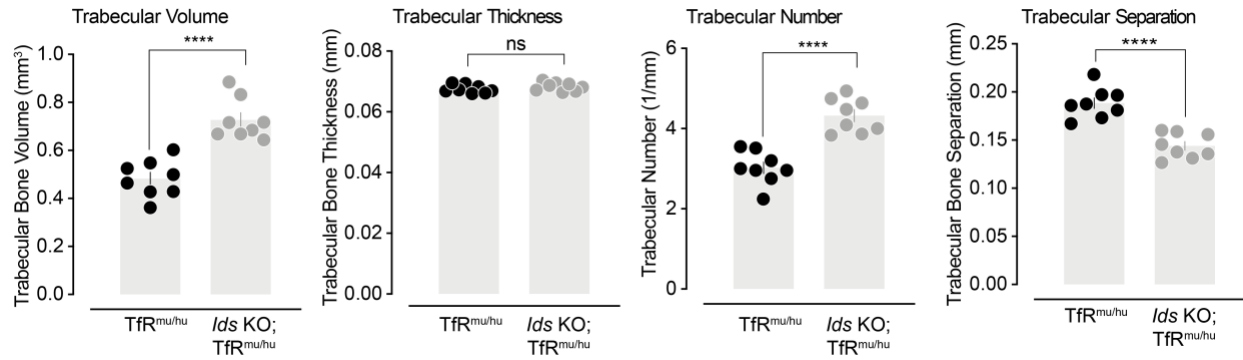
Supplemental Figure 3. ETV:IDS reduces microgliosis in the brain of *Ids* KO;TfR^{mu/hu} mice. Representative brain images from vehicle-treated TfR^{mu/hu} ($n = 5$), vehicle-treated *Ids* KO;TfR^{mu/hu} mice ($n = 5$), and ETV:IDS-treated *Ids* KO;TfR^{mu/hu} mice ($n = 5$). Microgliosis was assessed using coronal brain sections immunostained with antibodies against CD68 and imaged using a wide field fluorescence slide scanner. Scale bar: 200 μm.



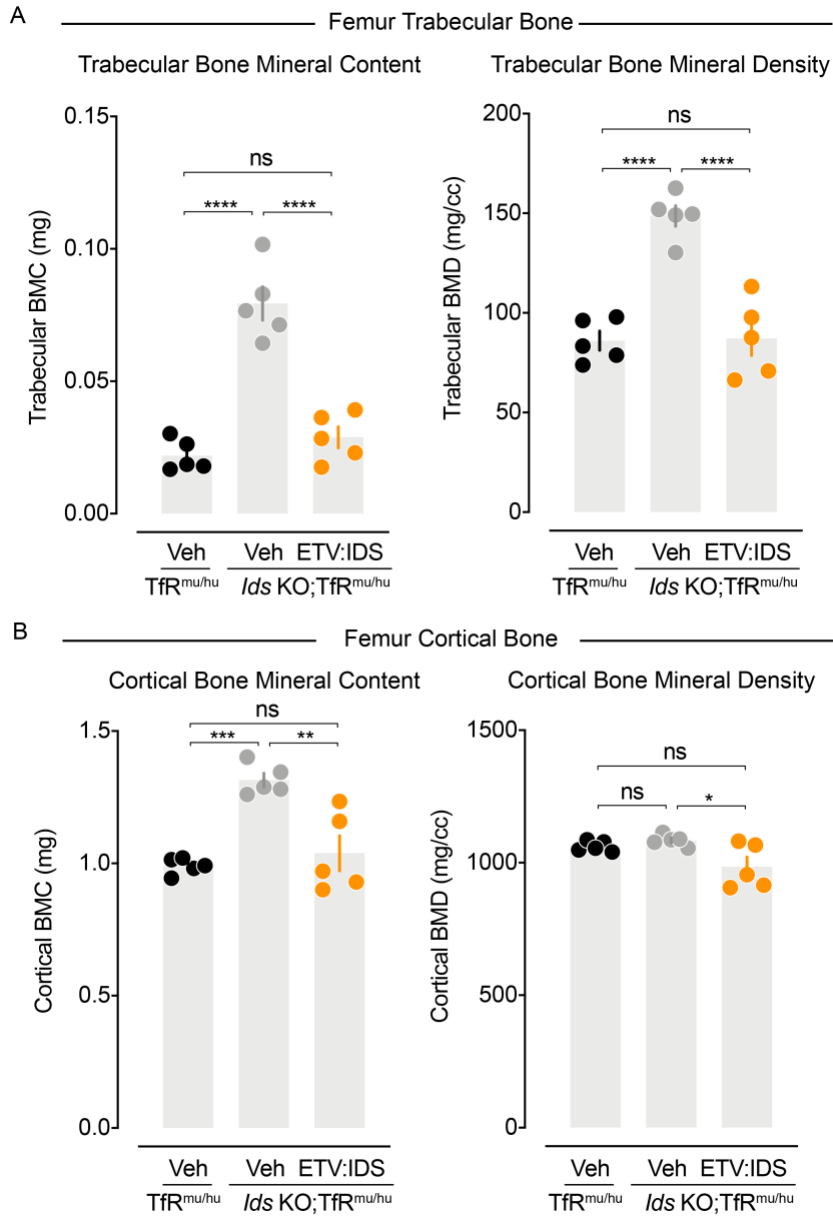
Supplemental Figure 4. Age-dependent increase in CSF Nf-L in *Ids* KO mice. (A) Nf-L levels were evaluated in the CSF from *Ids* KO ($n = 5$) and age-matched WT controls ($n = 3-5$). Graphs display mean \pm SEM: unpaired students t-test; * $p < 0.05$, ** $p < 0.01$, and *** $p < 0.001$.



Supplemental Figure 5. Behavioral phenotypes in *Ids* KO;*TfR*^{mu/hu} mice. We compared the performance of *Ids* KO;*TfR*^{mu/hu} ($n = 15$; gray) and *TfR*^{mu/hu} ($n = 15$; black) mice in several behavioral assays between 4 and 8 months of age. **(A)** Using the rotarod assay, the latency to fall during the training and testing trials was assessed; linear mixed-effects model, not significant. **(B)** Gait analysis including hind paw stance width and stride frequency was assessed on the treadmill assay at 15 cm/s; linear model, not significant. **(C)** The proportion of mice that successfully completed the running trials at each treadmill speed was assessed; Fisher's exact. **(D)** The level of pre-pulse inhibition of startle was assessed for each pre-pulse intensity; linear model. **(E)** In the active place avoidance assay, mice were trained to avoid an unmarked aversive zone where a mild foot shock was presented upon entrance in that zone. The number of entrances in the aversive zone was measured during each phase of testing; linear mixed-effects model. **(F)** The number of entrances in the aversive zone during the re-instatement trial was assessed; linear mixed effects model. **(G)** The classification of performance was based on the number of entrances in the aversive zone during the re-instatement trial; poor (>1), good (1), top (0); Fisher's exact test. All graphs display mean \pm SEM except contingency graphs in panels C and G. Comparison of genotype; * $p < 0.05$, ** $p < 0.01$ and **** $p < 0.0001$, ns = not significant.



Supplemental Figure 6. Skeletal phenotypes in *Ids* KO;TfR^{mu/hu} mice are present at treatment initiation. Micro-CT scans of the femur trabecular were performed from *Ids* KO;TfR^{mu/hu} and age-matched TfR^{mu/hu} controls at 4.5 months of age; $n = 8$ per group. Graphs display mean \pm SEM: unpaired students t-test; **** $p < 0.0001$, ns = not significant.



Supplemental Figure 7. ETV:IDS rescues skeletal abnormalities in *Ids* KO;*TfR*^{mu/hu} mice. Micro-CT scans of the (A) femur trabecular and (B) femur cortical bone was performed; *n* = 5 per group. BMC = bone mineral content, BMD = bone mineral density. Graphs display mean ± SEM: one-way ANOVA with Tukey's multiple comparison test; * *p* < 0.05, ** *p* < 0.01, *** *p* < 0.001, and **** *p* < 0.0001, ns = not significant.